Arch. Metall. Mater. **71** (2026), 2, 545-550

DOI: https://doi.org/10.24425/amm.2026.158838

MIJIN KIM[1], DONGWOON SHIN[1], TAEHO HA[1], DONGJU LEE[2], BYUNGHEON OH[2], PIL-HO LEE[1*]

PERFORMANCE ENHANCEMENT OF LCM-BASED ADDITIVELY MANUFACTURED MAGNETIC COMPOSITES VIA SPARK PLASMA SINTERING

This study explores spark plasma sintering (SPS) to improve the microstructural integrity and magnetic performance of NdFeB composite parts produced by lithography-based composites manufacturing (LCM). The composites, containing 84 wt.% NdFeB in a photosensitive polymer matrix, were magnetically aligned during printing using an in-situ field. SPS, applying pulsed current and uniaxial pressure under vacuum, was used to achieve densification while limiting grain growth. Samples were sintered at various temperatures with or without a magnetic field. Microstructure was examined via electron backscatter diffraction (EBSD) and X-ray diffraction (XRD), and magnetic properties were measured by Vibrating Sample Magnetometer (VSM). Optimized moderate-temperature, field-assisted sintering enhanced densification and magnetic anisotropy, whereas excessive sintering caused degradation. The combined use of in-situ magnetic alignment and SPS enables dense, anisotropic additively manufactured NdFeB composites with improved performance.

Keywords: Lithography-based composite manufacturing; Field-assisted additive manufacturing (FAAM); Anisotropic NdFeB magnets; Spark plasma sintering (SPS)

1. Introduction

The demand for magnetic materials has expanded significantly across industries such as transportation, energy, and electronics, driven by the miniaturization and complexity of modern devices [1]. Motors, sensors, and power generation systems increasingly rely on magnetic components with intricate geometries and robust properties [2]. However, conventional manufacturing methods like powder compaction and injection molding often fall short, especially when fine detail or internal cavities are required. As a result, additive manufacturing (AM) has emerged as a promising alternative for fabricating functional magnetic parts with high design freedom and tailored properties [3].

Magnetic materials are broadly classified into soft and hard magnetic types. Soft magnetic alloys, such as Fe-Si and Fe-Co, are preferred for their low coercivity and high permeability, enabling efficient energy transfer in transformers and inductors [4]. Conversely, hard magnetic materials like NdFeB and SmCo exhibit high coercivity and remanence, making them ideal for permanent magnets in motors and actuators [5]. AM research has explored both types, with soft magnetic printing focusing on minimizing losses and preserving permeability [6], and hard magnetic printing targeting particle alignment and enhanced remanence [7]. Progress has been made using laser-based processes such as Directed Energy Deposition (DED) and Powder Bed Fusion (PBF), although thermal input in these methods can degrade magnetic phases and diminish performance [8,9].

To mitigate thermal degradation and improve microstructural control, polymer-based printing techniques have drawn interest. Material extrusion (ME) supports high filler content but struggles with alignment and fine resolution [10-12]. Recently, vat photopolymerization (VPP) has shown potential with superior surface finish and geometry fidelity [13], though challenges remain, including light attenuation, particle sedimentation, and limited alignment retention in high-solid systems [14-15].

To address these issues, we employ a lithography-based composite manufacturing (LCM) process with in-situ magnetic alignment [16]. While this improves particle orientation, printed parts remain low in density due to the polymer matrix. Thus, we introduce spark plasma sintering (SPS) as a post-process to densify the composites. In this study, LCM-printed composites

[1] KOREA INSTITUTE OF MACHINERY AND MATERIALS, DEPARTMENT OF 3D PRINTING, DAEJEON, 156, GAJEONGBUK-RO, YUSEONG-GU, DAEJEON, 34103, REPUBLIC OF KOREA
[2] CHEONGJU, CHUNGBUK NATIONAL UNIVERSITY, DEPARTMENT OF URBAN, ENERGY, AND ENVIRONMENTAL ENGINEERING, REPUBLIC OF KOREA

* Corresponding author: pilho_lee@kimm.re.kr

with 84 wt.% NdFeB are sintered under varying thermal conditions. Microstructure and magnetic performance are evaluated via electron backscatter diffraction (EBSD) and X-ray diffraction (XRD), and Vibrating Sample Magnetometer (VSM) This work explores SPS as a means to enhance the density and magnetic properties of printed composites, supporting their future application in advanced magnetics.

2. Material and experimental details

An LCM-based AM system was used to fabricate highly filled magnetic composite specimens. The setup included a blade-type recoater for layer deposition, a DMD-based UV projection module, and an integrated magnetic alignment unit with dual permanent magnets for in-situ particle orientation. The build area was 75×135 mm^2 with a fixed layer thickness of 200 µm. A schematic of the system and processing flow is shown in Fig. 1.

The composite slurry was prepared by mixing a commercial acrylate-based resin with 35 wt.% HDDA as a reactive diluent and 5 wt.% TPO-L as a photoinitiator. Anisotropic NdFeB powder (80-150 µm, flake-like) was added at 84 wt.%, followed by 24 h of mechanical stirring and degassing to ensure uniform dispersion. Key printing parameters are summarized in TABLE 1.

Cube-shaped green parts were printed under two conditions: with and without in-situ magnetic alignment. These were sectioned into 10×10×10 mm^3 cubes for post-processing via SPS. SPS was conducted in vacuum using a graphite die under 40 MPa uniaxial pressure. The heating profile included ramping at 100°C/min, with two-step soaking: 5 min at 300°C for binder removal, and 5 min at either 750°C or 1000°C for densification. Joule heating and pressure were applied to achieve bonding while preserving alignment. The density increased from approximately 3.8 g/cm^3 in the green state to about 7.0-7.3 g/cm^3 after SPS, indicating significant densification. Four experimental conditions were tested, combining two alignment modes and two sintering temperatures. The detailed experimental conditions are summarized in TABLE 2.

Microstructure was characterized by EBSD on both surface and cross-sections. EBSD scans covered 1×1 mm^2 areas with 0.5 µm step size. Samples were mechanically polished using 0.04 µm colloidal silica. Magnetic properties were evaluated using a VSM, including coercivity, magnetization, retentivity, and squareness. Phase identification was conducted via XRD.

TABLE 1

Experimental conditions

Parameter	Value
Layer thickness	200 µm
Sample dimensions	10×10×10 mm^3
Recoating speed	60 mm/s
UV exposure time	15 sec/layer
Post-curing	UV light exposure 48 hr

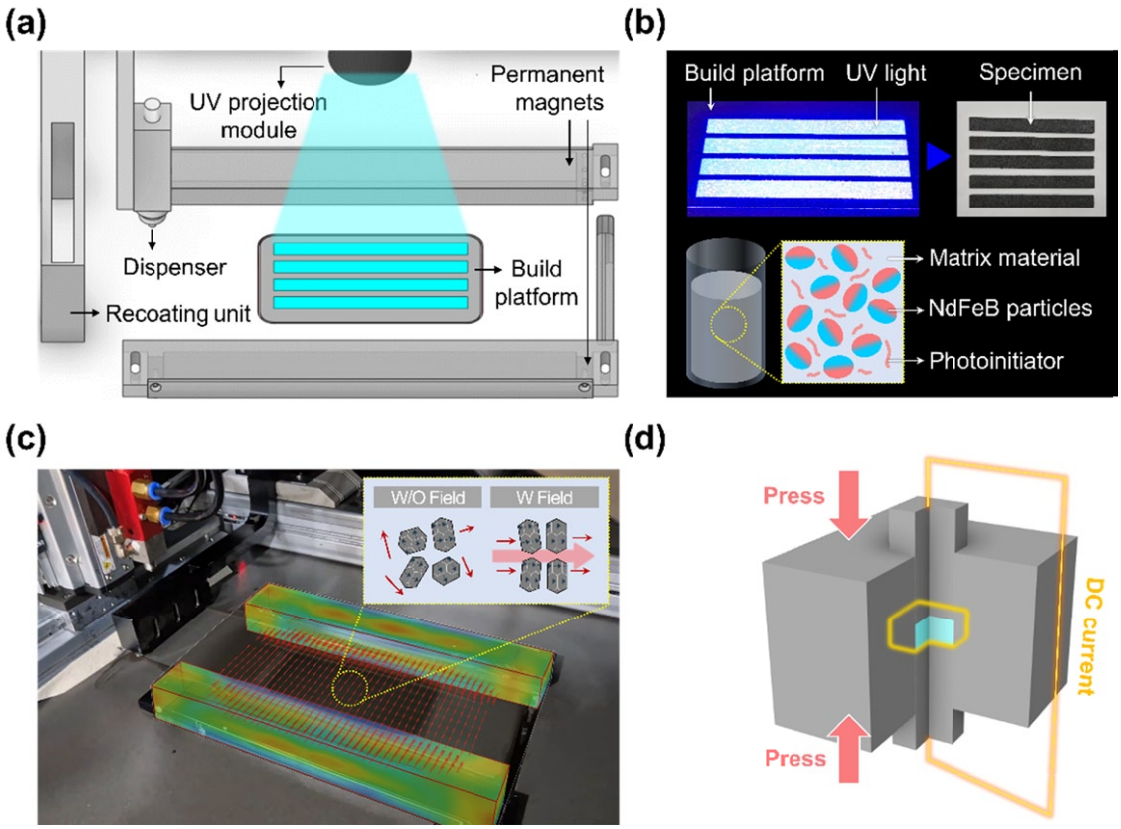

Fig. 1. Configuration of the developed LCM system (a) Configuration of the LCM-based additive manufacturing system (b) Depiction of the photocurable composite resin and layer fabrication process under UV illumination (c) design of the in-situ magnetic alignment module (d) schematic of the SPS process

TABLE 2

Experimental design

Run	Magnetic alignment	Densification temperature (°C)
1	Without field	750
2	Without field	1000
3	With field	750
4	With field	1000

3. Results and discussion

The magnetic and microstructural properties of the LCM-printed NdFeB composites were significantly affected by both the application of magnetic field alignment and the sintering conditions used during SPS post-processing. Fig. 2(a) shows the VSM hysteresis loops of the specimens, while Fig. 2(b) presents the quantitative comparison of their magnetic properties.

The coercivity (Hci) showed the highest value of 0.061 T for the specimen sintered at 750°C without a magnetic field, while it significantly decreased to 0.027 T when sintered at 1000°C. A similar decreasing trend was also observed under the magnetic field condition. In addition, the degradation in coercivity may also be partially associated with the formation of residual Fe phases, which reduce the effective volume of the hard magnetic NdFeB phase and interfere with magnetic domain alignment. The saturation magnetization (*Ms*) exhibited a noticeable enhancement under the magnetic alignment condition. The aligned specimens showed higher magnetization values, reaching 135 A·m^2/kg at 750°C, which is the highest among all samples. This improvement indicates that the directional orientation of anisotropic NdFeB particles induced during the LCM process was at least partially preserved throughout the SPS densification stage. The retentivity (*Mr*) showed a strong dependence on the sintering temperature, similar to the trend observed in coercivity. At 750°C, a moderate difference was found between the aligned and non-aligned specimens, whereas at 1000°C, both conditions exhibited a pronounced reduction in retentivity. The squareness ratio (*Mr*/*Ms*), which indicates the degree of magnetic alignment and the preservation of magnetic anisotropy, showed its highest value of 17% for the specimens sintered at 750°C with a magnetic field. It is noteworthy that the influence of sintering temperature appeared to be more significant than that of magnetic alignment itself. This tendency is consistent with the trend observed for the *Mr*, as the lower *Mr* values at 1000°C directly contributed to the reduction in the squareness ratio.

Overall, the specimens fabricated with an applied magnetic field and sintered at 750°C exhibited the most favorable magnetic performance among all conditions. This improvement can be attributed to the in-situ magnetic alignment induced during the LCM printing stage. In contrast, high-temperature sintering at 1000°C led to grain coarsening and reduced phase stability, resulting in the degradation of magnetic anisotropy. While densification improved with increasing temperature, excessive sintering led to a degradation of magnetic properties. This was evident in the reduced coercivity (*Hci*) and squareness ratio (*Mr*/*Ms*) observed in specimens sintered at 1000°C, which likely resulted from abnormal grain growth, deterioration of particle-matrix interfaces, or the formation of secondary phases. These results underline the importance of optimizing SPS process conditions – not only in terms of temperature and dwell time, but also to suppress the emergence of residual Fe phases that

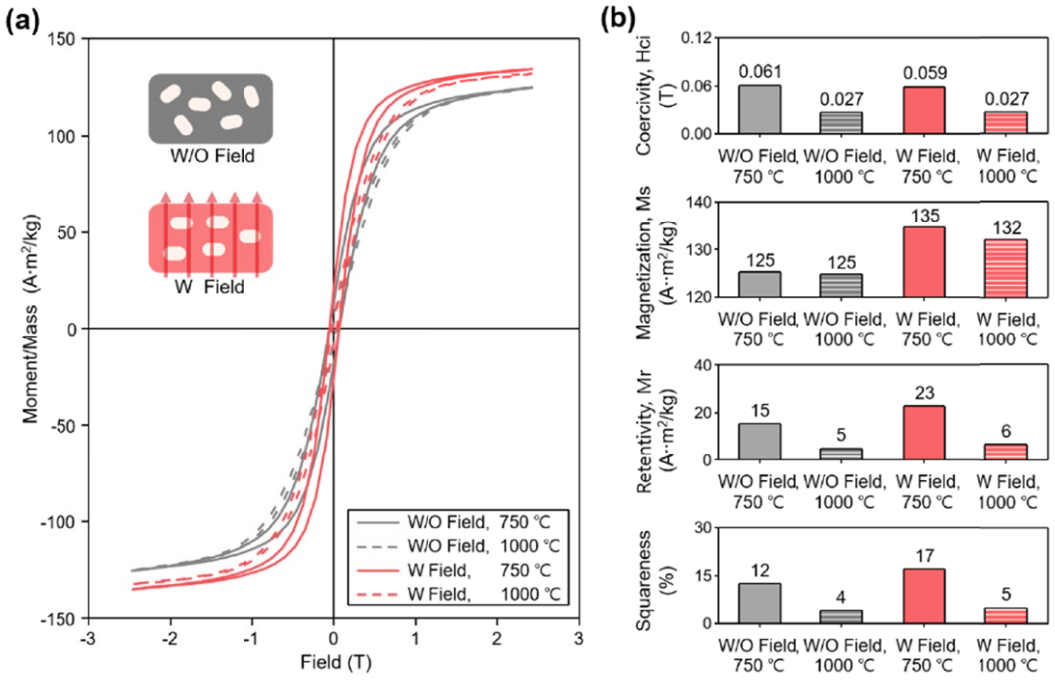

Fig. 2. Magnetic properties LCM-SPS fabricated NdFeB specimens (a) VSM hysteresis loops of LCM-SPS fabricated NdFeB specimens sintered at 750°C and 1000°C with and without an in-situ magnetic field (b) Quantitative analysis of magnetic properties obtained from the VSM hysteresis loops

can undermine the magnetic characteristics of the composite. These findings emphasize the need for careful control of sintering temperature and dwell time to balance densification and the retention of magnetic alignment.

To explore the microstructural origins of the observed magnetic behavior, EBSD analysis was conducted, and the results are summarized in Fig. 3. The EBSD maps reveal distinct variations in grain morphology and phase distribution depending on both the magnetic alignment and sintering temperature. Regardless of magnetic field application, the specimens sintered at 750°C exhibited a fine-grained microstructure with an average grain size of approximately 0.3 μm, characterized by uniformly distributed NdFeB grains and a relatively continuous phase network. In contrast, sintering at 1000°C led to pronounced grain coarsening, with some grains exceeding 40 μm in size, and a significant increase in ferrite phase formation. This microstructural coarsening, along with the development of a discontinuous NdFeB phase and a continuous ferrite network, is consistent with the observed reduction in Hci and squareness ratio at higher temperatures. The reduction in coercivity at higher temperatures may be attributed to grain growth during sintering, as confirmed by the EBSD results in Fig. 3, which indicate coarsening of microstructural features and reduced domain wall pinning. The relationship between grain refinement, magnetic alignment, and enhanced squareness ratio indicates that maintaining a fine-grained and directionally organized NdFeB phase is critical for improving magnetic performance. Nevertheless, the pronounced differences in textural and magnetic properties between aligned and non-aligned specimens confirm that structural anisotropy is the dominant factor governing the functional performance of the fabricated magnets. Together, the VSM and EBSD results validate the process strategy of combining in-situ magnetic alignment during LCM printing with the SPS process as an effective pathway for fabricating anisotropic magnetic composites.

X-ray diffraction analysis revealed a dominant peak near $2\theta \approx 44°$, which corresponds primarily to the $Nd_2Fe_{14}B$ (008) reflection associated with [001] texturing. However, this peak overlaps with the Fe (110) reflection, indicating the possible presence of residual iron phases. While the aligned specimen sintered at 750°C exhibited additional (00l) peaks such as (004), supporting the presence of [001] preferred orientation, further structural analysis is required to decouple the contribution from Fe. In specimens sintered at 1000°C, the appearance of additional Fe-related peaks – particularly Fe (200) near 65° and Fe (211) near 82.3° – suggests that high-temperature sintering may promote phase decomposition and Fe precipitation. Overall, the XRD results align with the VSM and EBSD findings, indicating that low-temperature sintering at 750°C helps retain the primary NdFeB phase and structural anisotropy, while higher temperatures induce microstructural instability and secondary phase formation.

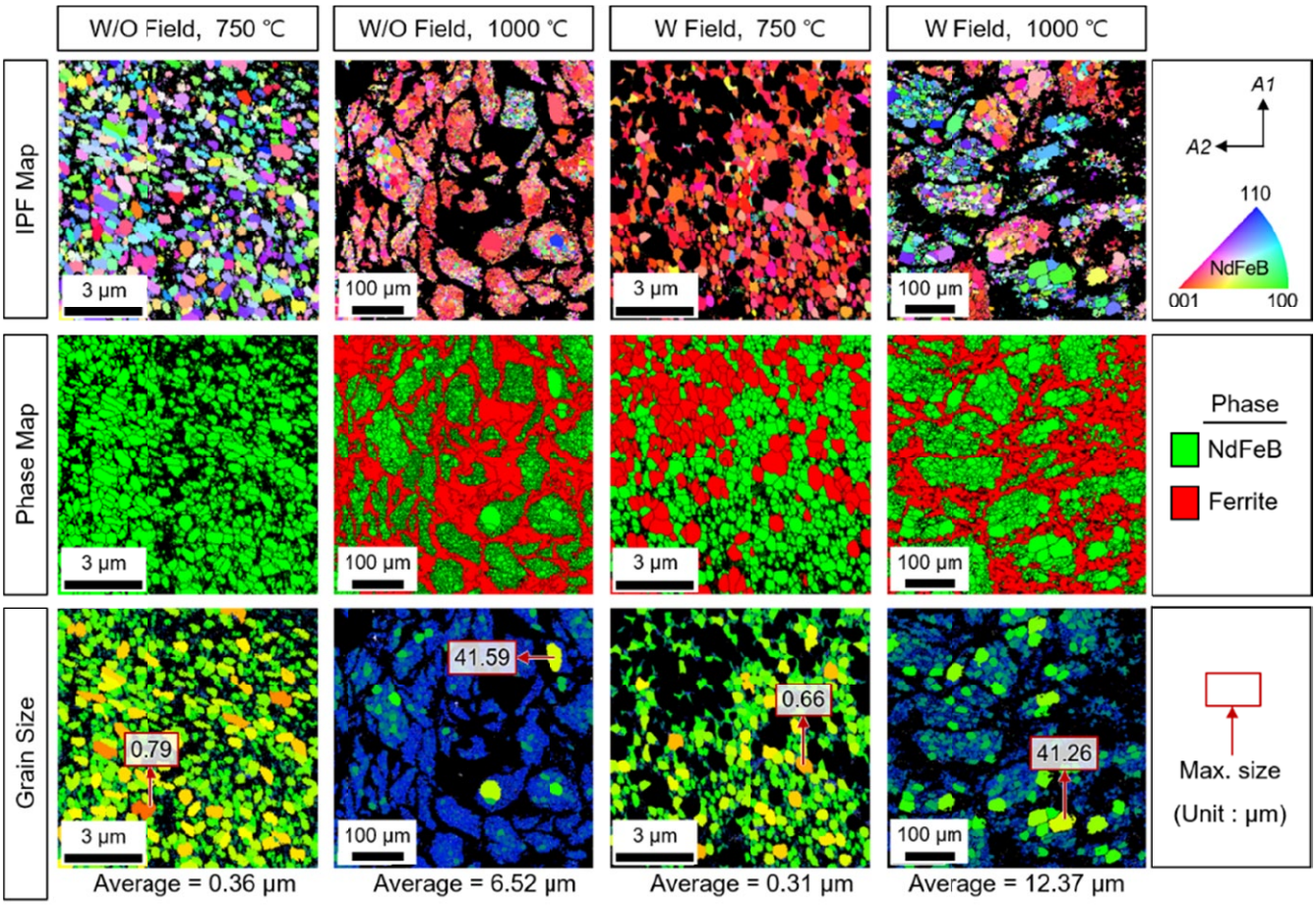

Fig. 3. EBSD maps of LCM-SPS fabricated NdFeB specimens

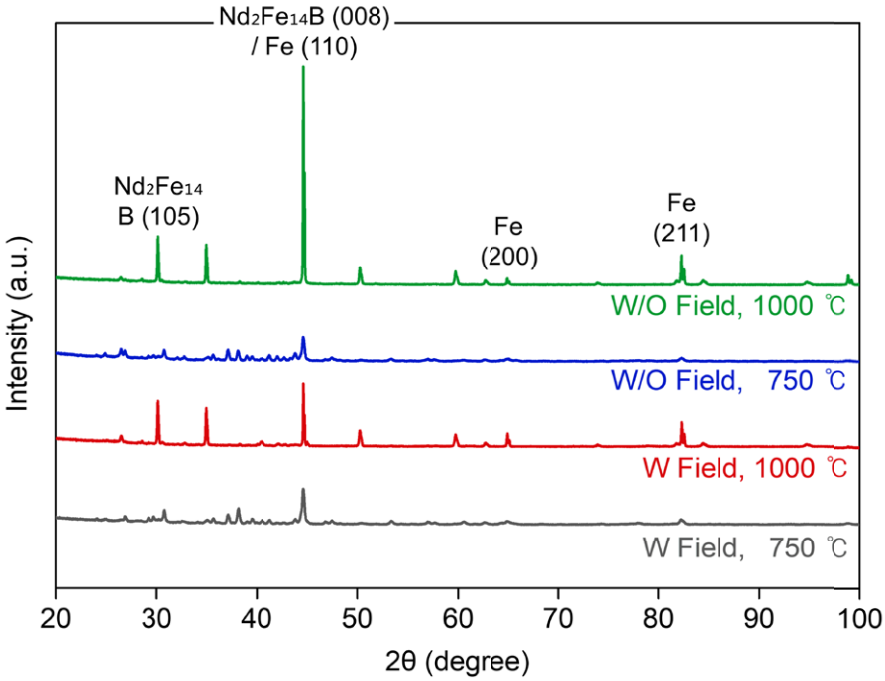

Fig. 4. XRD plot LCM-SPS fabricated NdFeB specimens

4. Conclusions

This study investigated the influence of magnetic field-assisted particle alignment and SPS post-processing on the microstructural and magnetic properties of highly filled NdFeB composites fabricated via an LCM-based additive manufacturing process. Anisotropic NdFeB particles were aligned under an in-situ magnetic field during the LCM process and subsequently consolidated using SPS under controlled conditions. VSM analysis revealed that specimens fabricated with magnetic field alignment and sintered at 750°C exhibited the highest Mr and squareness ratio, while excessive sintering at 1000°C led to a degradation of magnetic properties due to grain coarsening and secondary-phase formation.

EBSD analysis confirmed that the aligned specimens maintained a fine-grained and relatively continuous NdFeB phase network, whereas non-aligned and high-temperature-sintered specimens exhibited irregular and coarsened microstructures with discontinuous NdFeB regions and extensive ferrite formation. These microstructural features directly corresponded to the anisotropic magnetic performance observed in the VSM results.

While these results indicate a clear trend between magnetic alignment, sintering temperature, and magnetic anisotropy, the overall magnetic performance remains limited. XRD analysis suggests the presence of residual Fe phases, particularly in specimens sintered at 1000°C, which may contribute to phase decomposition and reduced anisotropy.

Therefore, this study should be considered a preliminary investigation, demonstrating the potential of combining in-situ magnetic alignment with SPS for processing anisotropic NdFeB composites. Further optimization of sintering atmosphere, temperature, and dwell time is required to improve phase stability and suppress secondary phase formation, thereby enabling reliable magnetic performance in future applications.

Acknowledgments

This work was supported by a grant of the Basic Research Program funded by the Korea Institute of Machinery and Materials (Grant No. NK255C), and the Technology Innovation Program (Grant No. 20024344) funded by the Ministry of Trade, Industry & Energy (MOTIE, Korea).

REFERENCES

[1] M. Randall, et al., Composites Reinforced in Three Dimensions by Using Low Magnetic Fields. Science **335**, 199-204. (2012).

[2] S. Tolbert, et al., Magnetic Field Alignment of Ordered Silicate-Surfactant Composites and Mesoporous Silica. Science **278**, 264-268 (1997).

[3] H. Zhai, et al., Review on the 3D Printing Technology and Application of Magnetic Materials: Material–Process–Structure–Application. Compos. Part B Eng. (2025), Article ID 112387. DOI: https://doi.org/10.1016/j.compositesb.2025.112387

[4] B. Yao, N. Kang, X. Li, D. Li, M. Mansori, J. Chen, H. Yang, H. Tan, X. Lin, Toward Understanding the Microstructure Characteristics, Phase Selection and Magnetic Properties of Laser Additive Manufactured Nd-Fe-B Permanent Magnets. Int. J. Extrem. Manuf. **6** (2023). DOI: https://doi.org/10.1088/2631-7990/ad0472

[5] E. Burzo, Permanent Magnets Based on R-Fe-B and R-Fe-C Alloys. Rep. Prog. Phys. **61**, 1099-1266 (1998). DOI: https://doi.org/10.1088/0034-4885/61/9/001

[6] L. Schäfer, et al., Design and Qualification of Pr–Fe–Cu–B Alloys for the Additive Manufacturing of Permanent Magnets. Adv. Funct. Mater. **31**, 2102148 (2021).
DOI: https://doi.org/10.1002/adfm.202102148

[7] L. Schäfer, et al., A Novel Magnetic Hardening Mechanism for Nd-Fe-B Permanent Magnets Based on Solid-State Phase Transformation. Adv. Funct. Mater. **33**, 2208821 (2022).
DOI: https://doi.org/10.1002/adfm.202208821

[8] H. Huckfeldt, et al., Selective Alignment of Molecular Glass Wrinkles by Engineered Magnetic Field Landscapes. Adv. Funct. Mater. **25**, 1503155 (2015).
DOI: https://doi.org/10.1002/adfm.201503155

[9] R. Mouhoubi, V. Lapinte, S. Blanquer, Programmable Liquid Crystal Elastomers Via Magnetic Field Assisted Oligomerization, Adv. Funct. Mater. **35**, 2424400 (2025).
DOI: https://doi.org/10.1002/adfm.202424400

[10] J. Yuan, et al., Alignment of Tellurium Nanorods via a Magnetization-Alignment-Demagnetization ("MAD") Process Assisted by an External Magnetic Field. ACS Nano. **3**, 1441-1450 (2009).
DOI: https://doi.org/10.1021/nn9002715

[11] X. Wei, M. Jin, H. Yang, X. Wang, Y. Long, Z. Chen, Advances in 3D Printing of Magnetic Materials: Fabrication, Properties, and Their Applications. J. Adv. Ceram. **11**, 665-701 (2022).
DOI: https://doi.org/10.1007/s40145-022-0567-5

[12] B. Rezaei, et al., Additive Manufacturing of Magnetic Materials for Energy, Environment, Healthcare, and Industry Applications. Adv. Funct. Mater. **35**, 2416823 (2024).
DOI: https://doi.org/10.1002/adfm.202416823

[13] W.C. Liu, V.H.Y. Chou, R. Behera, H.L. Ferrand, Magnetically Assisted Drop-on-Demand 3D Printing of Microstructured Multimaterial Composites. Nat. Commun. **13**, 5172 (2022).
DOI: https://doi.org/10.1038/s41467-022-32792-1

[14] J. Zhang, et al., Structure and Magnetic Properties of Nd-Fe-B/α-Fe Nanocomposite Magnets by Co, Nb, Dy Substitutions. J. Mater. Sci. Technol. **15**, 198-202 (1999).

[15] K.H. Ding, et al., High Energy and High Coercivity Sintered NdFeB Magnets by Low Oxygen Process. J. Mater. Sci. Technol. **16**, 127-128 (2009).

[16] M. Kim, H. Lee, D. Shin, J.P. Choi, T. Ha, J.P. Jeun, P.H. Lee, Magnetic alignment and electron beam post-curing of NdFeB materials via lithography-based composite manufacturing. Virtual Phys. Prototyp. e2593543 (2025).
DOI: https://doi.org/10.1080/17452759.2025.2593543